J Physiol 595.15 (2017) pp 5129–5142

The Journal of Physiology

Kir2.1 and K2P1 channels reconstitute two levels of resting membrane potential in cardiomyocytes

Dongchuan Zuo[1], Kuihao Chen[1], Min Zhou[2], Zheng Liu[3] and Haijun Chen[1]

[1] *Department of Biological Sciences, University at Albany, State University of New York, Albany, NY, USA*
[2] *Department of Neuroscience, The Ohio State University Wexner Medical Center, Columbus, OH, USA*
[3] *Department of Cardiology, Shanghai Tenth People's Hospital, Tongji University School of Medicine, Shanghai, China*

Key points

- Outward and inward background currents across the cell membrane balance, determining resting membrane potential. Inward rectifier K^+ channel subfamily 2 (Kir2) channels primarily maintain the resting membrane potential of cardiomyocytes.
- Human cardiomyocytes exhibit two levels of resting membrane potential at subphysiological extracellular K^+ concentrations or pathological hypokalaemia, however, the underlying mechanism is unclear.
- In the present study, we show that human cardiomyocytes derived from induced pluripotent stem cells with enhanced expression of isoform 1 of Kir2 (Kir2.1) channels and mouse HL-1 cardiomyocytes with ectopic expression of two pore-domain K^+ channel isoform 1 (K2P1) recapitulate two levels of resting membrane potential, indicating the contributions of Kir2.1 and K2P1 channels to the phenomenon.
- In Chinese hamster ovary cells that express the channels, Kir2.1 currents non-linearly counterbalance hypokalaemia-induced K2P1 leak cation currents, reconstituting two levels of resting membrane potential.
- These findings support the hypothesis that Kir2 currents non-linearly counterbalance inward background cation currents, such as K2P1 currents, accounting for two levels of resting membrane potential in human cardiomyocytes and demonstrating a novel mechanism that regulates excitability.

Abstract Inward rectifier K^+ channel subfamily 2 (Kir2) channels primarily maintain the normal resting membrane potential of cardiomyocytes. At subphysiological extracellular K^+ concentrations or pathological hypokalaemia, human cardiomyocytes show both hyperpolarized and depolarized resting membrane potentials; these depolarized potentials cause cardiac arrhythmia; however, the underlying mechanism is unknown. In the present study, we show that inward rectifier K^+ channel subfamily 2 isoform 1 (Kir2.1) currents non-linearly counterbalance hypokalaemia-induced two pore-domain K^+ channel isoform 1 (K2P1) leak cation currents, reconstituting two levels of resting membrane potential in cardiomyocytes. Under hypokalaemic conditions, both human cardiomyocytes derived from induced pluripotent stem cells with enhanced Kir2.1 expression and mouse HL-1 cardiomyocytes with ectopic expression of K2P1 channels recapitulate two levels of resting membrane potential. These cardiomyocytes display N-shaped current–voltage relationships that cross the voltage axis three times and the first and third zero-current potentials match the two levels of resting membrane potential. Inhibition of K2P1 expression eliminates the phenomenon, indicating contributions of Kir2.1 and K2P1 channels to two levels of resting membrane potential. Second, in Chinese hamster ovary cells that heterologously express the channels, Kir2.1 currents non-linearly counterbalance hypokalaemia-induced K2P1 leak cation currents, yielding the N-shaped current–voltage relationships, causing the resting membrane potential to spontaneously jump from

DOI: 10.1113/JP274268

hyperpolarization at the first zero-current potential to depolarization at the third zero-current potential, again recapitulating two levels of resting membrane potential. These findings reveal ionic mechanisms of the two levels of resting membrane potential, demonstrating a previously unknown mechanism for the regulation of excitability, and support the hypothesis that Kir2 currents non-linearly balance inward background cation currents, accounting for two levels of resting membrane potential of human cardiomyocytes.

(Received 3 March 2017; accepted after revision 22 May 2017; first published online 24 May 2017)
Corresponding author H. Chen: Department of Biological Sciences, University at Albany, State University of New York, Albany, NY 12222, USA. Email: hchen01@albany.edu

Abbreviations CHO, Chinese hamster ovary; iPSC, induced pluripotent stem cells; *I–V*, current–voltage; Kir2, inward rectifier K^+ channel subfamily 2; Kir2.1, inward rectifier K^+ channel subfamily 2 isoform 1; K2P1, two pore-domain K^+ channel isoform 1; NMDG, *N*-methyl-D-glucamine; PFU, plaque-forming units.

Introduction

Inward rectifier K^+ channel subfamily 2 (Kir2) channels medicate the I_{K1} background K^+ currents and regulate electrical excitability (Hibino *et al.* 2010). Although the resting membrane potential is determined by the balance of outward and inward background ionic currents across the cell membrane, Kir2 channels are primarily responsible for the maintenance of normal resting membrane potentials of cardiomyocytes and cardiac Purkinje fibres (Lopatin & Nichols, 2001), which are close to the K^+ equilibrium potential, usually around −90 mV. At subphysiological extracellular K^+ concentrations ($[K^+]_e$) or pathological hypokalaemia, in which blood K^+ concentrations decrease to 1.5 to 3 mM (Rastegar & Soleimani, 2001), human cardiomyocytes (Ten Eick & Singer, 1979; McCullough *et al.* 1987; McCullough *et al.* 1990) and cardiac Purkinje fibres of human, sheep and canines (Weidmann, 1956; Ellis, 1977; Gadsby & Cranefield, 1977; Miura *et al.* 1977; Lee & Fozzard, 1979; Sheu *et al.* 1980; Christe, 1982; Shah *et al.* 1987) can have two stable levels of resting membrane potential: one at hyperpolarization more negative than −80 mV and the other at depolarization more positive than −40 mV. The depolarization of the two levels of resting membrane potential causes cardiac arrhythmia (Zaza, 2009; Goldstein, 2011). The phenomenon of the two stable levels of resting membrane potential is also observed in other multiple types of cells, including skeletal muscle cells and macrophages, at physiological or pathological $[K^+]_e$ (Gallin, 1981; Geukes Foppen *et al.* 2002; Struyk & Cannon, 2008; Jurkat-Rott *et al.* 2009). Such unusual electrical behaviours have been studied extensively from 1956 onward, however, the mechanism underlying this well-known phenomenon is not well understood.

Cardiac Purkinje fibres have N-shaped current–voltage (*I–V*) relationships that cross the voltage axis three times, and the first and third zero-current potentials determine the two levels of resting membrane potential (Gadsby & Cranefield, 1977; Carmeliet *et al.* 1987). Kir2 channels are essential for the N-shaped *I–V* relationships because these channels primarily maintain the resting membrane potential and have a conductance region with a negative slope (Gadsby & Cranefield, 1977; Shah *et al.* 1987; Hibino *et al.* 2010). How Kir2 channels contribute to the two levels of resting membrane potential is unknown (Struyk & Cannon, 2008). It has also been assumed that inward Na^+ currents contribute to the two levels of resting membrane potential of cardiac Purkinje fibres because external Na^+ is required (Gadsby & Cranefield, 1977; Lee & Fozzard, 1979; Sheu *et al.* 1980). Indeed, large inward leak Na^+ currents are observed in cardiac Purkinje fibres and human spherical primary cardiac myocytes in K^+-free bath solutions (Eisner & Lederer, 1979*b*, *a*; Ma *et al.* 2011*b*). We recently discovered that cardiac two pore-domain K^+ channel isoform 1 (K2P1) (Lesage *et al.* 1996; Goldstein *et al.* 2005; Rajan *et al.* 2005) conducts such inward leak Na^+ currents because K2P1 channels dynamically change ion selectivity and become non-selective cation channels at a subphysiological $[K^+]_e$ (Ma *et al.* 2011*b*). However, the inward leak Na^+ current cannot explain observations such as the all-or-none depolarization of the resting membrane potential (Goldstein, 2011).

In the present study, we investigated the mechanisms that result in two levels of resting membrane potential of cardiomyocytes at subphysiological $[K^+]_e$ or moderate and severe hypokalemic conditions. We focused on cardiac background or leak channels that are regulated by a reduction of physiological $[K^+]_e$. Kir2 channels are inhibited by reduction of normal $[K^+]_e$ (Hibino *et al.* 2010). K2P1 channels are highly expressed in the human heart (Gaborit *et al.* 2007) and switch to conduct inward leak cation (mainly Na^+) currents at subphysiological $[K^+]_e$ (Ma *et al.* 2011*b*). Therefore, we investigated the contributions of Kir2 and K2P1 channels to the two levels of resting membrane potential by employing human cardiomyocytes derived from human induced pluripotent stem cells (iPSC-derived cardiomyocytes) that conduct small I_{K1} or Kir2 currents (Doss *et al.* 2012; Hoekstra

et al. 2012; Lieu *et al.* 2013), mouse HL-1 cardiomyocytes that do not express K2P1 channels (Claycomb *et al.* 1998; Ma *et al.* 2011*b*) and mammalian heterologous expression systems Chinese hamster ovary (CHO) cells.

At subphysiological $[K^+]_e$, both human iPSC-derived cardiomyocytes engineered to overexpress inward rectifier K^+ channel subfamily 2 isoform 1 (Kir2.1) and mouse HL-1 cardiomyocytes that ectopically express human K2P1 channels recapitulated two levels of resting membrane potential and displayed N-shaped *I–V* relationships that intersect the voltage axis three times, with the first and third zero-current potentials determining the two levels of resting membrane potential. Second, we confirmed that Kir2 and K2P1 channels reconstitute the two levels of resting membrane potential and N-shaped *I–V* relationships when heterologously expressed in CHO cells. Our analyses reveal the mechanism of how two levels of resting membrane potential are generated, demonstrate a unique mechanism of regulation of excitability, and support the hypothesis that Kir2 currents balance non-linearly opposing background cation currents, such as K2P1 leak cation currents, setting up two levels of resting membrane potential of human cardiomyocytes at subphysiological $[K^+]_e$.

Methods

Ethical approval

The present study did not involve animal experiments or human experiments. Our experiments comply with the policies and regulations oulined in Grundy (2015).

Constructs and adenoviruses

The human sequence encoding Kir2.1 (AF153820) was synthesized and cloned into the pUC57 vector (GenScript Corporation, Piscataway, NJ, USA) at the *Eco*RV site. The inserts encoding human Kir2.1, K2P1 and K2P1•T118I sequences were then subcloned into pDUAL-CCM(–) shuttle vector (Vector BioLabs, Malvern, PA, USA) via *Xho*1 and *Bam*H1 sites. These cDNAs were then cloned into the pAd vectors in which GFP or mCherry reporter expression is driven by its own cytomegalovirus promoter. We previously validated the use of human K2P1 shRNA #1 (targeting sequence: GCACATCATAGAGCATGACCAACTGTCCT) in human spherical cardiac myocytes (Ma *et al.* 2011*b*). A cassette containing the U6 promoter and hK2P1 shRNA #1 sequence in pRFP-C-RS vectors (TF315498; Origene, Rockville, MD, USA) was subcloned into the pDUAL-Basic shutter vector (Vector BioLabs) at *Eco*RI and *Hind*III restriction sites and then into pAd-GFP vectors (Vector BioLabs). Validated human K2P1 shRNA #5 (targeting sequence: TCAGAGAGCTCTATAAGATTG, SKU#: shADV-212731; Vector BioLabs) and control ineffective shRNA sequences (catalogue number 1122; Vector BioLabs) were synthesized and cloned into the vector pAd-GFP-U6-shRNA. All constructs were confirmed by automated DNA sequencing.

Adenovirus construction, purification and titration were performed by Vector Biolabs. Viral particles of Ad-mCherry-hKir2.1, Ad-GFP-hK2P1, Ad-GFP-hK2P1•T118I, Ad-GFP-hK2P1 shRNA #1, Ad-GFP-hK2P1 shRNA #5 and Ad-GFP control shRNA were obtained at concentrations in the order of 10^{10} plaque-forming units (PFU) ml^{-1}. mCherry and GFP allowed the identification of transduced cells. Viral particles were diluted 100-fold with Dulbecco's modified Eagle's medium, aliquoted and stored at −80°C.

Cell culture and transduction

Mouse HL-1 cardiomyocytes and CHO cells were cultured as described previously (Ma *et al.* 2011*b*). Briefly, mouse HL-1 cardiomyocytes and CHO cells were maintained in Claycomb medium supplemented with 10% fetal bovine serum and Dulbecco's modified Eagle's medium supplemented with 10% fetal calf serum, respectively, in a 5% CO_2 incubator. CHO cells were seeded on glass cover slips in 35 mm dishes 24 h before transduction. Cells of 60% to 80% confluence were transduced with adenovirus particles of Ad-mCherry-hKir2.1 alone, Ad-GFP-hK2P1 (or T118I) alone and both Ad-mCherry-hKir2.1 and Ad-GFP-hK2P1 (or T118I) (1:1 ratio) at concentrations of 1.8–3.1 × 10^7 PFU ml^{-1}. Mouse HL-1 cardiomyocytes were seeded on gelatin-coated glass cover slips and transduced with viral particles. Many of cultured HL-1 cardiomyocytes did not have a normal resting membrane potential of around −80 mV in 5 mM $[K^+]_e$ and we confirmed that these HL-1 cardiomyocytes had very small I_{K1} currents, implying that they express endogenous Kir2 channels at low levels. Thus, we standardized HL-1 cardiomyocytes with overexpression of Kir2.1 channels so that every tested HL-1 cardiomyocyte had a normal resting membrane potential at physiological $[K^+]_e$.

Human iPSC-derived cardiomyocytes (CMC-100-110-001) were purchased from Cell Dynamic International (Madison, WI, USA) and cultured in a 37°C, 5% CO_2 incubator in accordance with the manufacturer's instructions. Human iPSC-derived cardiomyocytes were transduced after culture for 8–20 days, and electrophysiological studies were performed 2 days after viral transduction. Briefly, human iPSC-derived cardiomyocytes were first seeded on gelatin-coated glass coverslips in 12-well culture plates at density of 40 000 cells $well^{-1}$ with iCell Cardiomyocyte Plating Medium (CMM-100-110-001; Cell Dynamic International), which was replaced by iCell Cardiomyocyte Maintenance Medium (CMM-100-120-001; Cell

Dynamic International) 48 h later. The maintenance medium was then changed every 2 days. For shRNA-mediated inhibition of K2P1 expression, human iPSC-derived cardiomyocytes cultured in three parallel dishes were transduced with Ad-GFP-hK2P1 shRNA #1, Ad-GFP-hK2P1 shRNA #5 or Ad-GFP-scrambled shRNA at a concentration of 1.8–3.1 $\times$ 10^5 PFU ml^{-1}. For other electrophysiological experiments, human iPSC-derived cardiomyocytes were transduced with Ad-mCherry-hKir2.1 alone at a concentration of 2.7 $\times$ 10^5 PFU ml^{-1}.

Western blotting analysis

Human iPSC-derived cardiomyocytes or CHO cells transfected with human K2P1 channels were harvested by aspirating the medium and washing twice with PBS. Cells were then suspended in 1 ml of PBS and centrifuged. Isolated cell pellets were lysed with modified RIPA buffer (50 mM Tris-HCl, 150 mM NaCl, 0.1% SDS, 1% Triton X-100, 1% sodium deoxycholate, 1 mM EGTA and protease inhibitors) for 30 min on ice. Cell lysates were then centrifuged at 12 000 *g* for 20 min at 4°C. After transferring the supernatant to a fresh ice-cold tube, protein was quantified with the BCA protein assay kit (Pierce, Rockford, IL, USA). Equal concentrations of proteins were mixed with SDS sample buffer and denatured at 95°C for 5 min. Total protein samples (20 μg) were resolved on a 10% SDS-PAGE gel and transferred to polyvinylidene fluoride membranes. The membranes were blocked with 5% non-fat milk in TTBS (50 mM Tris, 500 mM NaCl and 0.1% Tween 20) for 1 h. Membranes were then incubated with primary antibodies directed against K2P1 (dilution 1:800; Alomone, Jerusalem, Israel) or GAPDH (dilution 1:1000; Santa Cruz Biotechnology, Santa Cruz, CA, USA) overnight at 4°C. After washing with TTBS, the membranes were incubated with HRP-conjugated secondary antibodies (dilution 1:5000; Santa Cruz Biotechnology) for 1 h. The membranes were washed again with TTBS and then the blots were analysed using an enhanced chemiluminescence detection system (Bio-Rad, Hercules, CA, USA).

Electrophysiology

Recordings of membrane potentials and whole-cell currents were performed with the EPC-10 USB amplifier and a Dell 745 computer (Dell, Round Rock, TX, USA) with PatchMaster software (HEKA Elektronik, Lambrecht, Germany). Electrophysiological recordings were performed with whole-cell patch clamp configurations at a sampled rate of 2 KHz and data were analysed as described previously (Ma *et al.* 2011*b*). Patch pipettes with resistances of 2.0–3.5 MΩ were used. Series resistances are small than 10 MΩ. Series resistance was compensated at least 80% to minimize voltage errors. Whole-cell ramp currents were recorded with a standard 2.2 s voltage ramp from −140 mV to +80 mV each 15 s with voltage clamp techniques. Membrane potentials were continuously recorded with current clamp techniques during changes of bath solutions. We did not correct for small changes of liquid junction potentials, which resulted from the switch between Na^+- and $NMDG^+$ (*N*-methyl-D-glucamine)-based bath solutions. To control the quality of recordings on leak or background K^+ channels, we only analysed data from experiments with membrane resistances of at least 1 GΩ at resting membrane potential and check reversal potentials of whole-cell ramp currents at the beginning of recordings. Electrophysiological data were analysed with FithMaster (HEKA Elektronik), IGOR Pro (WaveMetrics, Portland, OR, USA) and Excel (Microsoft Corp., Redmond, WA, USA). All data are reported as the mean ± SEM. Two-tailed Student's *t* tests were used to evaluate significance of differences between two groups of data.

For electrophysiological recordings in CHO cells, the pipette solution contained 140 mM KCl, 1 mM $MgCl_2$, 10 mM EGTA, 1 mM K_2-ATP and 5 mM Hepes (pH 7.4) and the bath solution contained 135 mM NaCl, 5 mM KCl, 2 mM $CaCl_2$, 1 mM $MgCl_2$, 15 mM glucose and 10 mM Hepes (pH 7.4). For electrophysiological recordings in human iPSC-derived cardiomyocytes and mouse HL-1 cardiomyocytes, the pipette solution contained 20 mM KCl, 120 mM potassium aspartate, 1 mM $MgCl_2$, 5 mM Na_2-ATP, 0.5 mM Na_2-GTP, 10 mM EGTA and 5 mM Hepes (pH 7.4) and the bath solution contained 140 mM NaCl, 5.4 mM KCl, 1.8 mM $CaCl_2$, 1 mM $MgCl_2$, 10 mM glucose and 10 mM Hepes (pH 7.4). To block voltage-gated Ca^+ currents in cardiomyocytes, 2 mM $CoCl_2$ was added to bath solutions. For CHO cells and cultured cardiomyocytes, 5 mM and 5.4 mM $[K^+]_e$ were used, respectively. The total concentration of Na^+ and K^+ in bath solutions was kept constant and so Na^+-based bath solutions with various $[K^+]_e$ were obtained by increasing or decreasing K^+ and replacing it with equimolar Na^+. $NMDG^+$-based bath solutions with indicated $[K^+]_e$ were obtained by replacing extracellular Na^+ with equimolar $NMDG^+$.

Results

Human iPSC-derived cardiomyocytes with enhanced Kir2.1 expression recapitulate two levels of resting membrane potential at subphysiological $[K^+]_e$

We first examined the contribution of Kir2 channels to two levels of resting membrane potential of cardiomyocytes. Commercially available human iPSC-derived cardiomyocytes are well characterized and have been used in biomedical research (Ma *et al.* 2011*a*; Karakikes *et al.* 2015). These cells have ionic currents that are

quantitatively similar to those reported for human adult cardiomyocytes with the exception of Kir2 currents (Doss *et al.* 2012; Hoekstra *et al.* 2012; Lieu *et al.* 2013). Human iPSC-derived cardiomyocytes have a resting membrane potential that is significantly depolarized (around −60 mV) compared to that of human adult cardiomyocytes (approximately −80 mV) because the iPSC-derived cardiomyocytes have small Kir2 currents. Enhanced expression of Kir2.1 channels or 'electronic expression' of I_{K1} currents suffices to mature action potential profiles of human iPSC-derived cardiomyocytes (Bett *et al.* 2013; Lieu *et al.* 2013). Thus, human iPSC-derived cardiomyocytes function in a manner similar to human adult cardiomyocytes in which Kir2 channel expression is significantly reduced. We enhanced Kir2.1 expression in iPSC-derived cardiomyocytes via the viral transduction of the gene encoding Kir2.1 to study impact of Kir2 channels on resting membrane potential.

We monitored resting membrane potentials and background currents of Kir2.1-expressing human iPSC-derived cardiomyocytes as $[K^+]_e$ was decreased. All cells analysed had one level of resting membrane potential of −71.7 ± 0.1 mV (n = 196) in 5.4 mM $[K^+]_e$. When $[K^+]_e$ was reduced to 1 mM, conditions in which human cardiomyocytes and cardiac Purkinje fibres often show two stable levels of resting membrane potential (Gadsby & Cranefield, 1977; McCullough *et al.* 1990), Kir2.1-expressing human iPSC-cardiomyocytes rapidly hyperpolarized to −106.2 ± 0.5 mV (n = 196) in phase 1 because the resting membrane potential followed the Nernst equation as a result of Kir2 channel function. Reduced Kir2 currents counterbalance low $[K^+]_e$–induced cation currents, so the cardiomyocytes exhibited three distinct behaviours with respect to resting membrane potential in phase 2. The first subset, ∼35% of the cells, remained hyperpolarized at −108.3 ± 0.6 mV (n = 68) and had typical I_{K1}-like whole-cell currents with a reversal potential of −109.3 ± 0.8 mV (Fig. 1*A*), implying that Kir2 currents still dominated.

A second population, 19% of the cells, recapitulated the classical two stable levels of resting membrane potential observed in cardiac Purkinje fibres and human cardiomyocytes (Christe, 1982; McCullough *et al.* 1990). These cells spontaneously depolarized to −15.3 ± 1.0 mV (n = 38) in an all-or-none fashion and then remained

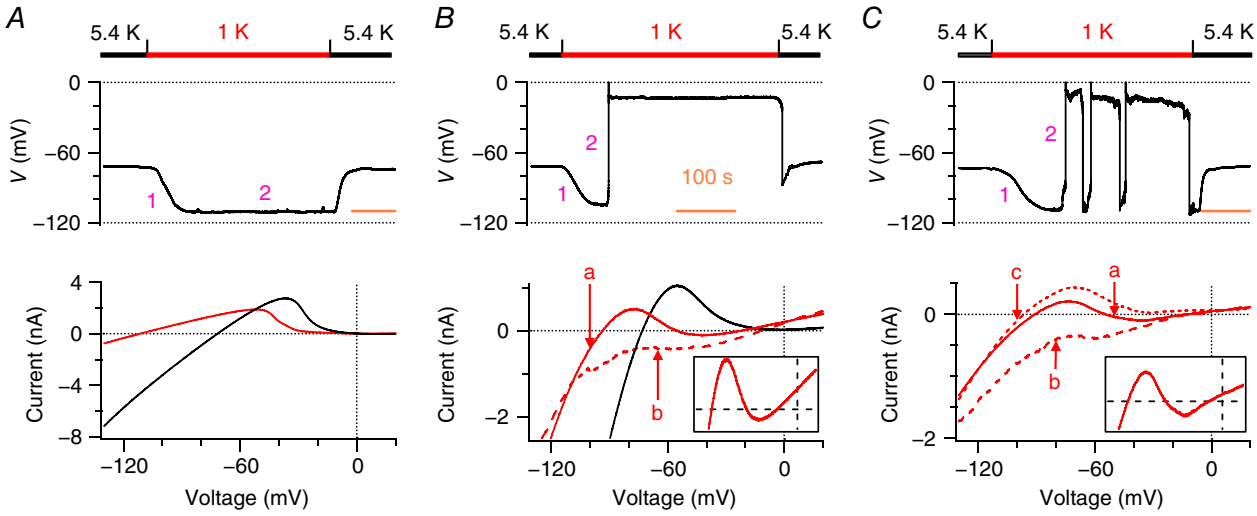

Figure 1. Human iPSC-derived cardiomyocytes with enhanced expression of Kir2.1 recapitulate two levels of resting membrane potential in 1 mM $[K^+]_e$
A–C, resting membrane potentials (top) and whole-cell ramp currents (bottom) of human iPSC-derived cardiomyocytes, which were transduced with Kir2.1 viral particles, are shown when Na^+-based bath solutions were reversibly changed from 5.4 mM K^+ (black bars) to 1 mM K^+ (red bars). Representatives of three populations of cells are shown. *A*, 35% of cells remained on hyperpolarization. *B*, 19% of the cells recapitulated the classical two stable levels of resting membrane potential. *C*, 46% of cells spontaneously depolarized and then fluctuated between hyperpolarization and depolarization. Top: membrane potentials were continuously recorded during changes of bath solutions; pink numbers 1 and 2 represent phases 1 and 2 of changes in membrane potentials, respectively. Time scale (orange bars) = 100 s. Bottom: *I–V* relationships are shown by whole-cell ramp currents, which were measured in the cells showing the same changes in membrane potentials. Black lines represent currents recorded in 5.4 mM $[K^+]_e$; solid red lines represent '*a*' type N-shaped ramp currents; bold dash red lines represent '*b*' type ramp currents with a depolarized reversal potential; thin dash red lines represent '*c*' type ramp currents with a hyperpolarized reversal potential (n = 5–196). Inserts: magnifications of the N-shaped ramp currents (between −110 and 20 mV; from −200 to 300 pA), illustrating clearly the three zero-current potentials.

at this depolarization for more than 300 s until $[K^+]_e$ was returned to 5.4 mM (Fig. 1*B*, top). The transition from hyperpolarization to depolarization was permanent, so that the cells had two stable levels of resting membrane potential. This subgroup of the cells mainly showed '*a*' type N-shaped whole-cell ramp currents that intersected with the voltage axis three times, similar to that previously observed in cardiac Purkinje fibres (Gadsby & Cranefield, 1977). The first and third zero-current potentials (-97.5 ± 4.5 mV; -15.8 ± 0.7 mV, $n = 6$) had a positive slope conductance and determined the two levels of resting membrane potential. These cells also simultaneously or separately displayed '*b*' type whole-cell ramp currents with a reversal potential of -18.6 ± 5.1 mV ($n = 5$), comparable to the third zero-current potentials of the N-shaped ramp currents (Fig. 1*B*, bottom).

The largest subset, 46% of Kir2.1-expressing human iPSC-derived cardiomyocytes, spontaneously depolarized to -18.8 ± 0.8 mV ($n = 90$) from hyperpolarization and then fluctuated between hyperpolarization and depolarization (Fig. 1*C*, top). Spontaneous transitions from hyperpolarization to depolarization were temporary in this population as if the injection of small outward currents switched depolarization back to hyperpolarization. Such fluctuating resting membrane potentials have not been reported in human cardiomyocytes or in cardiac Purkinje fibres at subphysiological $[K^+]_e$, however, fluctuating resting membrane potentials do occur in macrophages (Gallin, 1981; Gallin & Livengood, 1981) and osteoclasts (Ravesloot *et al.* 1989; Sims & Dixon, 1989) at physiological $[K^+]_e$. This population of Kir2.1-expressing human iPSC-derived cardiomyocytes showed '*a*' N-shaped whole-cell ramp currents with first and third zero-current potentials of -99.0 ± 2.9 mV and -16.8 ± 1.8 mV ($n = 15$), respectively, '*b*' type whole-cell ramp current with a reversal potential of -17.1 ± 1.9 mV ($n = 17$) and also an additional '*c*' type whole-cell ramp current with a reversal potential of -103.7 ± 1.8 ($n = 18$) matching the first zero-current potentials of the N-shaped ramp currents (Fig. 1*C*, bottom). These cells had very dynamic whole-cell ramp currents, consistent with their fluctuating resting membrane potentials. The same cells often dynamically displayed all three types of currents, depending on fluctuation patterns of resting membrane potential. The dynamic currents reflected resting membrane potentials that spontaneously fluctuate between the two levels or that remain depolarized or hyperpolarized.

We also studied Kir2.1-expressing human iPSC-derived cardiomyocytes in $[K^+]_e$ that occurs under moderate and severe hypokalaemia. When $[K^+]_e$ was decreased to 2 mM, the cells hyperpolarized to -94.4 ± 0.4 mV ($n = 160$) in phase 1. In phase 2, 12% the cells exhibited classical two stable levels of resting membrane potential and permanently depolarized to -18.9 ± 1.7 mV ($n = 19$). About 23% of the cells showed spontaneous fluctuation of resting membrane potential between -93.2 ± 0.8 mV and -19.9 ± 1.3 mV ($n = 37$). As observed in 1 mM $[K^+]_e$, the first population of the cells displayed '*a*' and '*b*' types of whole-cell ramp current, and the second population was dynamic with '*a*', '*b*' and '*c*' types of whole-cell ramp current. The first and third zero-current potentials (-87.9 ± 2.5; -19.0 ± 1.9 mV, $n = 15$) of '*a*' type N-shaped whole-cell ramp currents determined the two levels of resting membrane potential. The remaining 65% of the cells remained hyperpolarized at around -95 mV as a result of dominant Kir2 currents. In 2.7 mM $[K^+]_e$, only 7% of Kir2.1-expressing human iPSC-derived cardiomyocytes showed resting membrane potentials that spontaneously fluctuated between -83.9 ± 3.2 mV and -19.1 ± 5.5 mV ($n = 4$); the remainder stayed hyperpolarized at -87.0 ± 0.3 mV ($n = 56$). Therefore, human iPSC-derived cardiomyocytes with enhanced Kir2.1 expression recapitulated two stable levels of resting membrane potential that are observed in human adult cardiomyocytes and cardiac Purkinje fibres. It is worth noting that only a fraction of the iPSC-derived cardiomyocytes showed such a phenomenon, consistent with previous observations in human adult cardiomyocytes (Christe, 1982; McCullough *et al.* 1990). The iPSC-derived cardiomyocytes had a greater probability of showing two levels of resting membrane potential at lower subphysiological $[K^+]_e$, implying that they may conduct larger, low $[K^+]_e$-induced inward cation currents, such as K2P1 cation currents, at lower subphysiological $[K^+]_e$.

K2P1 channels contribute to two levels of resting membrane potential in Kir2.1-expressing human iPSC-derived cardiomyocytes in 2 mM $[K^+]_e$

We examined the contributions of inward Na^+ currents to two levels of resting membrane potential of Kir2.1-expressing human iPSC-derived cardiomyocytes in 2 mM $[K^+]_e$ because resting membrane potential is determined by the balance of Kir2 currents and opposing cation currents. Replacement of external Na^+ with equimolar $NMDG^+$ reversibly shifted resting membrane potentials from a depolarization of -22.8 ± 2.2 mV ($n = 5$) to a hyperpolarization of -92.6 ± 1.3 mV. Only the '*c*' type whole-cell ramp current was found in $NMDG^+$-based bath solutions, whereas the same cells exhibited '*a*' type N-shaped whole-cell ramp currents in Na^+-based bath solutions (Fig. 2*A*). Removal of inward Na^+ currents thus eliminates both the N-shaped currents and the two levels of resting membrane potential in the cardiomyocytes.

We next isolated the contributions of K2P1 channels and K2P1 leak cation currents to two levels of resting membrane potential in Kir2.1-expressing human

iPSC-derived cardiomyocytes in 1 or 2 mM $[K^+]_e$. The low $[K^+]_e$-induced K2P1 leak cation currents are one of major background cation currents that balance Kir2 currents and determine resting membrane potentials (Ma *et al.* 2011*b*). Human iPSC-derived cardiomyocytes express K2P1 channels as shown by analysis of K2P1 proteins (Fig. 2*B*) and by demonstration of the presence of quinine-sensitive K2P1-like inward leak Na^+ currents in 0 mM $[K^+]_e$ (Fig. 2*C*). These K2P1 leak Na^+ currents were previously characterized with cloned K2P1 channels (Ma *et al.* 2011*b*). We performed two sets of experiments for this purpose. First, at a test voltage of −80 mV, of the 24 iPSC-derived cardiomyocytes showing two levels of resting membrane potential in 1 mM $[K^+]_e$, 18 cells conducted K2P1-like inward leak Na^+ currents of -757 ± 129 pA ($n = 18$) in 0 mM $[K^+]_e$. The remaining six of these 24 cells did not conduct K2P1-like inward leak Na^+ currents, implying that other inward cation currents contribute to the two levels of resting membrane potential. Indeed, previous reports imply that inward Ca^{2+} flux may contribute to the two levels of resting membrane potential of cardiac Purkinje fibres in K^+-free and Na^+-free bath solutions (Wiggins & Cranefield, 1976). By contrast, the iPSC-derived cardiomyocytes that did not show two levels of resting membrane potential conducted K2P1-like inward leak Na^+ currents of -160 ± 71 pA ($n = 9$) at −80 mV in 0 mM $[K^+]_e$, which are much smaller currents than those observed in the iPSC-derived cardiomyocytes showing two levels of resting membrane potential.

Second, we studied Kir2.1-expressing human iPSC-derived cardiomyocytes from which K2P1 was depleted using an RNAi approach because specific blockers of K2P1 channels are not available. We used two previously validated K2P1-specific shRNAs (Ma *et al.* 2011*b*), which, in human spherical primary cardiomyocytes, decrease K2P1 expression by 70%. Less than 10% of the iPSC-derived cardiomyocytes that expressed K2P1-specific shRNA had two levels of resting membrane potential in 2 mM $[K^+]_e$, whereas 35% of the iPSC-derived cardiomyocytes that expressed control shRNA showed the phenomenon (Fig. 2*D*). These results imply that K2P1 leak currents are the major background cation currents in ∼75% of Kir2.1-expressing human

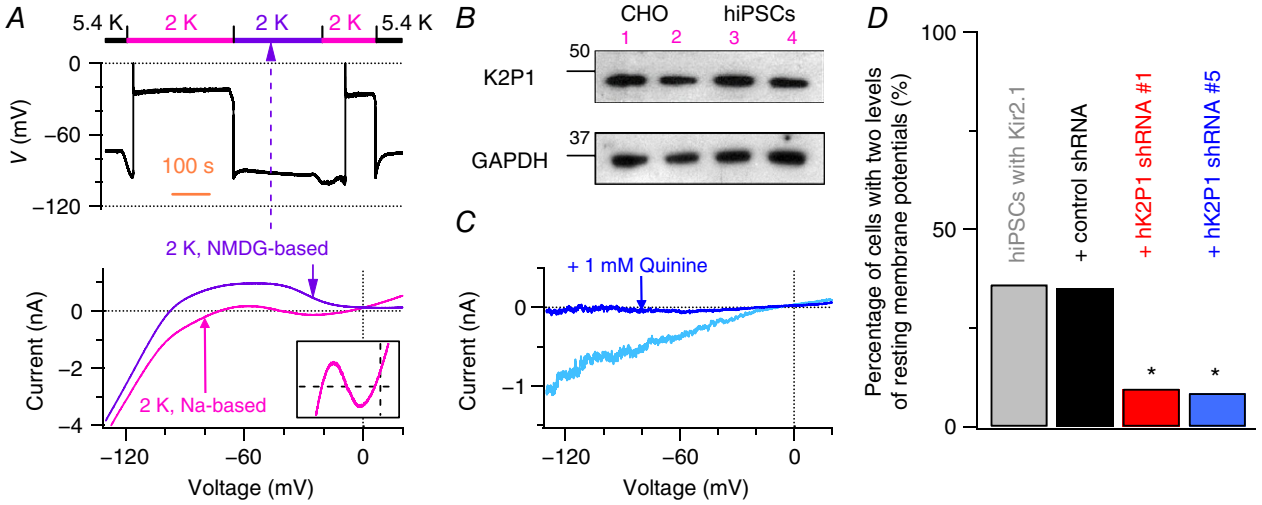

Figure 2. K2P1 leak cation currents contribute to two levels of resting membrane potential in Kir2.1-expressing human iPSC-derived cardiomyocytes in 2 mM $[K^+]_e$
A, removal of external Na^+ eliminates both the two levels of resting membrane potential and N-shaped *I–V* relationships in Kir2.1-expressing human iPSC-derived cardiomyocytes. Top: resting membrane potentials were monitored when Na^+-based bath solutions were first changed from 5.4 to 2 mM K^+, then reversibly moved to $NMDG^+$-based solutions with 2 mM K^+ (purple bar), and eventually returned to 5.4 mM K^+. Bottom: whole-cell ramp currents were measured before and after external Na^+ was replaced by equimolar $NMDG^+$. Insert: magnification of whole-cell ramp currents (between −100 and 20 mV; from −200 to 300 pA). *B*, K2P1 proteins detected in human iPSC-derived cardiomyocytes (hiPSCs, lanes 3 and 4) by western blot analysis. Proteins isolated from CHO cells transduced with human K2P1 channels served as positive controls (lanes 1 and 2). We did not observe this K2P1 band in proteins isolated from control CHO cells, when we initially validated the K2P1-specific antibody. GAPDH was detected as a loading control. *C*, quinine-sensitive K2P1-like inward leak Na^+ currents in 0 mM $[K^+]_e$. Whole-cell ramp currents of Kir2.1-expressing human iPSC-derived cardiomyocytes were recorded before (blue line) and after (teal line) application of 1 mM quinine, a non-specific K^+ channel blocker. *D*, percentage of Kir2.1-expressing human iPSC-derived cardiomyocytes (without and with expression of indicated shRNAs) that showed two levels of resting membrane potential in 2 mM $[K^+]_e$. $^*P = 0.0001$, relative to control ineffective shRNA; $n = 114$ to 160 cells for each group from 11 experiments.

iPSC-derived cardiomyocytes that show the two levels of resting membrane potential.

Mouse HL-1 cardiomyocytes with ectopic expression of K2P1 channels recapitulate two levels of resting membrane potential at subphysiological $[K^+]_e$

We also confirmed the contribution of K2P1 channels to two levels of resting membrane potential of cardiomyocytes by analysis of resting membrane potentials and background currents of mouse HL-1 cardiomyocytes engineered to express human K2P1 channels. Mouse HL-1 cardiomyocytes that lack of K2P1 expression do not show two levels of resting membrane potential at subphysiological $[K^+]_e$ (Ma *et al.* 2011*b*). We used mouse HL-1 cardiomyocytes that ectopically express human K2P1•T118I mutant channels as negative controls because the T118I mutation eliminates dynamic ion selectivity of K2P1 channels and K2P1•T118I mutant channels do not conduct inward leak Na^+ currents at subphysiological $[K^+]_e$ (Ma *et al.* 2011*b*; Chatelain *et al.* 2012).

In 5.4 mM $[K^+]_e$, mouse HL-1 cardiomyocytes that expressed K2P1 or K2P1•T118I channels had a resting membrane potential of around −73 mV. When $[K^+]_e$ was reduced to 1 mM, mouse HL-1 cardiomyocytes that express K2P1•T118I mutant channels simply hyperpolarized to −108.9 ± 1.0 mV (n = 21), consistent with reversal potentials (−108.7 ± 1.5 mV) of the whole-cell ramp currents (Fig. 3*A*). By contrast, mouse HL-1 cardiomyocytes that expressed K2P1 channels experienced a short hyperpolarization to −106.8 ± 0.5 mV (n = 164) in phase 1 and showed the three different types of behaviours with respect to resting membrane potential in phase 2 that were observed in Kir2.1-expressing human iPSC-derived cardiomyocytes. The first population, 53% of the HL-1 cells (n = 87), stayed hyperpolarized because Kir2 currents dominated and overcame K2P1 currents (Fig. 3*B*). However, 18% of the HL-1 cells showed classical two levels of resting membrane potential. These cells spontaneously depolarized to and then remained at −24.8 ± 1.4 mV (n = 29) (Fig. 3*C*). Both '*a*' and '*b*' types of currents were observed in this subset of cells. The remainder of the HL-1 cells (29%) showed

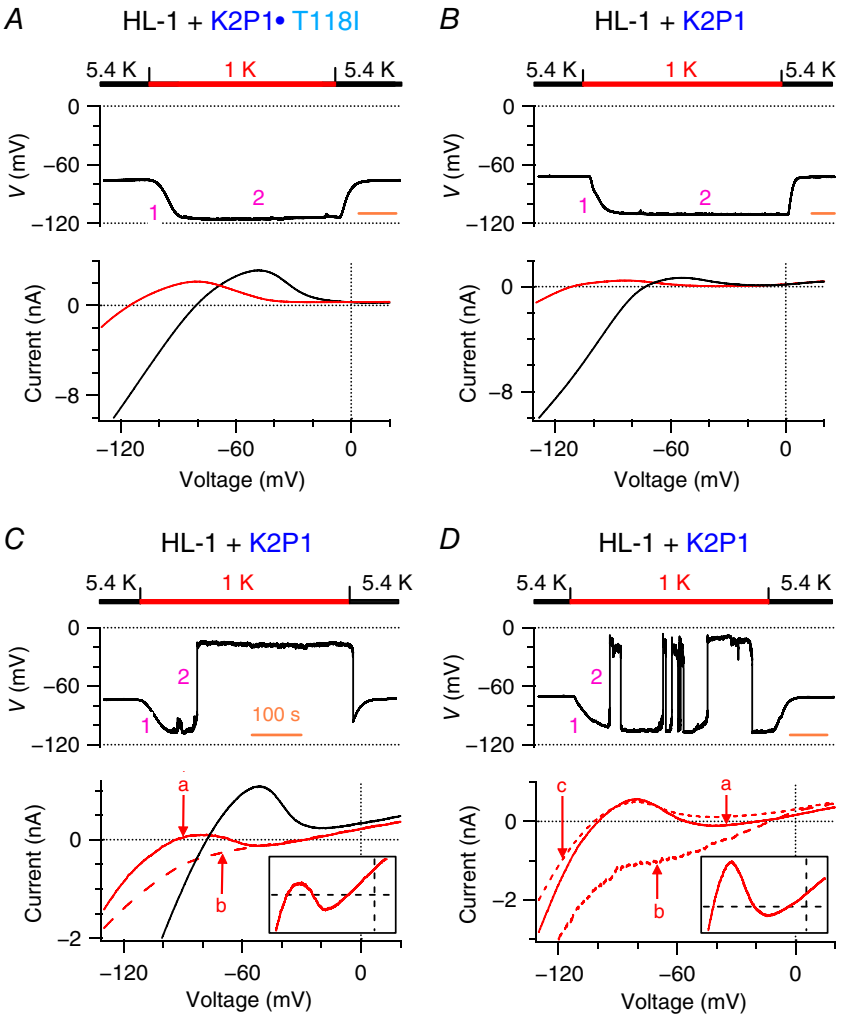

Figure 3. Mouse HL-1 cardiomyocytes with ectopic expression of K2P1 channels recapitulate two levels of resting membrane potential in 1 mM $[K^+]_e$
A–D, resting membrane potentials (top) and whole-cell ramp currents (bottom) of mouse HL-1 cardiomyocytes that express human K2P1•T118I (*A*) or human K2P1 (*B–D*) channels when Na^+-based bath solutions were reversibly changed from 5.4 to 1 mM K^+ (n = 6–68 per group). *B–D* are representative of three populations of cells that show three different phenotypes on resting membrane potentials described in Fig. 1. The '*a*', '*b*' and '*c*' in (*C*) and (*D*) represent three types of whole-cell ramp currents described in Fig. 1. The '*b*' and '*c*' currents have reversal potentials of −27.8 ± 2.3 mV (n = 18) and −105.6 ± 0.8 mV (n = 24), respectively. Inserts: magnifications of whole-cell ramp currents between −300 and 300 pA at test voltages between −110 and 20 mV. Time scale (orange bars) = 100 s.

spontaneous fluctuation of resting membrane potentials between −108.9 ± 0.6 and −27.5 ± 1.0 mV (n = 48) and '*a*', '*b*' and '*c*' types of whole-cell ramp current were observed (Fig. 3*D*). In these latter two subgroups of the cells, the first and third zero-potentials (−98.1 ± 2.2 mV; −26.7 ± 2.0 mV, n = 15) of '*a*' type N-shaped ramp currents were stable and determined two levels of resting membrane potential.

In 2.7 mM $[K^+]_e$, 21% of the HL-1 cells permanently shifted to −25.7 ± 3.3 mV (n = 13) from −87.1 ± 1.6 mV, whereas 13% of the HL-1 cardiomyocytes spontaneously fluctuated between −87.9 ± 1.1 mV (n = 11) and −22.8 ± 2.4 mV in phase 2. These cells also displayed '*a*' type N-shaped ramp currents with the first and third zero-current potentials of −80.6 ± 1.3 mV and −20.2 ± 2.6 mV (n = 9), respectively. The percentage of the HL-1 cardiomyocytes exhibiting two levels of resting membrane potential was lower in 2.7 mM $[K^+]_e$ than in 1 mM $[K^+]_e$, consistent with the fact that K2P1 channels dynamically change ion selectivity and conduct low $[K^+]_e$-induced inward cation currents in a $[K^+]_e$-dependent manner (Ma *et al.* 2011*b*).

When external Na^+ was replaced with equimolar $NMDG^+$ in 1 mM $[K^+]_e$, the HL-1 cardiomyocytes were reversibly shifted from a classical depolarization of −26.4 ± 1.9 mV (n = 21) to a hyperpolarization of −96.7 ± 1.9 mV, and fluctuation between the two levels was eliminated (Fig. 4*A* and *B*). The '*a*' and '*b*' types of whole-cell ramp current disappeared, and only '*c*' type currents with single reversal potentials of −100.6 ± 3.1 mV (n = 6) were recorded (Fig. 4*C*). The two groups of the HL-1 cardiomyocytes showing the two levels of resting membrane potential conducted large quinine-sensitive K2P1 inward Na^+ currents in 0 mM $[K^+]_e$, which were not observed in mouse HL-1 cardiomyocytes that expressed the K2P1•T118I channels (Fig. 4*D*). These experiments confirmed the contribution of K2P1 inward leak Na^+ currents to the two levels of resting membrane potential and N-shaped ramp currents in the HL-1 cardiomyocytes.

Kir2.1 and K2P1 channels reconstitute two levels of resting membrane potential in transduced CHO cells at subphysiological $[K^+]_e$

Finally, we confirmed the contributions of Kir2.1 and K2P1 channels to the two levels of resting membrane potential and examined how Kir2.1 currents

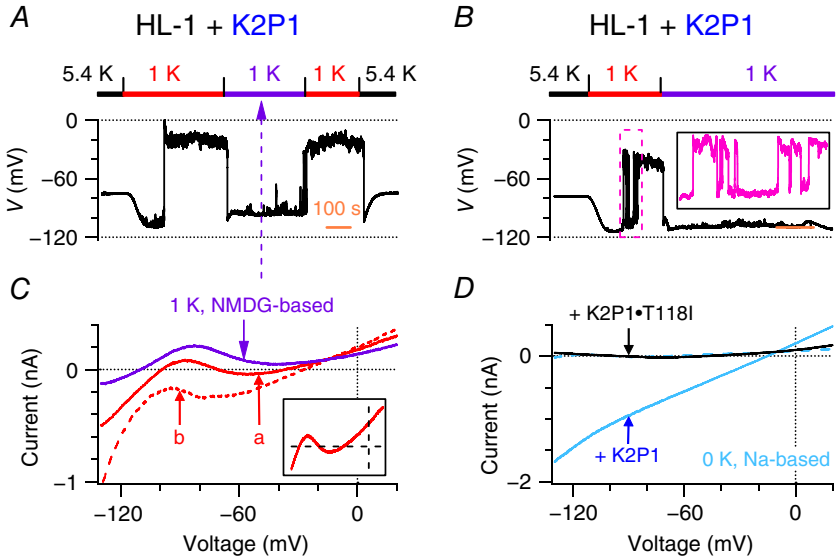

Figure 4. K2P1 leak cation currents contribute to two levels of resting membrane potential in mouse HL-1 cardiomyocytes with ectopic expression of K2P1 in 1 mM $[K^+]_e$
A–B, representative resting membrane potentials of two populations of mouse HL-1 cardiomyocytes that express human K2P1 channels and display the two levels of resting membrane potential when Na^+-based bath solutions were first changed from 5.4 to 1 mM K^+ and then reversibly shifted to $NMDG^+$-based bath solutions with 1 mM K^+ (purple bars). Insert: magnification of the pink box. Time scale (orange bars) = 100 s. *C*, representative whole-cell ramp currents of these mouse HL-1 cardiomyocytes were recorded before (solid and dashed red lines) and after (purple line) external Na^+ was replaced by equimolar $NMDG^+$ in bath solutions with 1 mM K^+. The '*a*' and '*b*' represent two types of dynamic whole-cell ramp currents described in Fig. 1. Insert: magnification of whole-cell ramp currents between −200 and 300 pA at test voltages between −110 and 20 mV. *D*, representative whole-cell ramp currents of mouse HL-1 cardiomyocytes that express K2P1 (teal line) or K2P1•T118I (black line) channels in K^+-free Na^+-based bath solutions. Dashed teal line indicates the K2P1-like inward leak Na^+ current that was blocked by 1 mM quinine.

counterbalance K2P1 leak cation currents and maintain resting membrane potential in transduced CHO cells in 1 and 2.7 mM $[K^+]_e$. We confirmed that Kir2.1 currents decreased and K2P1 channels switched to conduct leak cation currents by analysis of CHO cells that expressed either Kir2.1 or K2P1 in response to changes of $[K^+]_e$ from 5 to 1 mM (Fig. 5*A*). The CHO cells that expressed both Kir2.1 and K2P1 channels had a resting membrane potential of -77.3 ± 0.3 mV ($n = 96$) in 5 mM $[K^+]_e$ because both Kir2.1 and K2P1 channels function as background K^+ channels that maintain resting membrane potentials to follow the Nernst equation for K^+. When $[K^+]_e$ was lowered to 1 mM, the CHO cells rapidly hyperpolarized to around -110 mV in phase 1. Subsequently, reduced Kir2.1 outward K^+ currents began to re-balance low $[K^+]_e$-induced K2P1 leak cation currents, determining resting membrane potential in phase 2. When Kir2.1 outward K^+ currents dominated, the CHO cells remained hyperpolarized at -111.1 ± 1.0 mV ($n = 31$), consistent with reversal potentials (-112.0 ± 2.1 mV) of their whole-cell ramp currents (Fig. 5*B*). These CHO cells did express K2P1 channels because quinine-sensitive K2P1 inward leak Na^+ currents were identified when $[K^+]_e$ was further lowered to 0 mM ($n = 6$).

By contrast, when Kir2.1 outward K^+ currents did not absolutely overcome K2P1 inward leak cation currents,

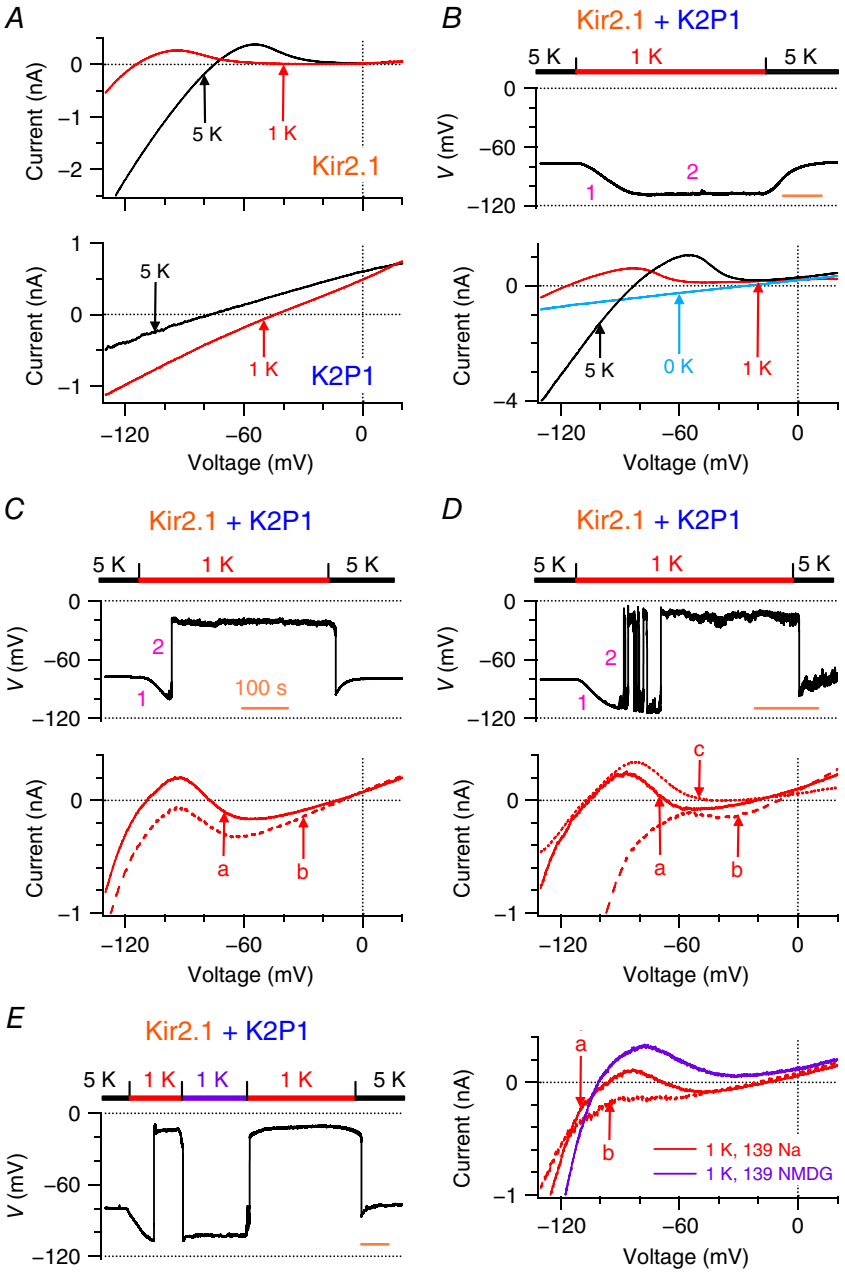

Figure 5. Kir2.1 and K2P1 channels reconstitute two levels of resting membrane potential in transduced CHO cells in 1 mM $[K^+]_e$
A, representative whole-cell ramp currents in CHO cells engineered to express human Kir2.1 channels (top) or human K2P1 channels (bottom) before and after Na^+-based bath solutions were changed from 5 mM (black lines) to 1 mM (red lines) K^+. Reversal potentials of Kir2.1 and K2P1 currents in 1 mM $[K^+]_e$ are -110.5 ± 1.5 mV ($n = 7$) and -46.4 ± 2.9 mV ($n = 8$), respectively. *B–D*, representative resting membrane potentials (top) and whole-cell ramp currents (bottom) of three populations of CHO cells that express both Kir2.1 and K2P1 channels are shown when Na^+-based bath solutions were reversibly changed from 5 to 1 mM K^+ ($n = 6$–49 per group). These cells showed three different phenotypes on resting membrane potentials described in Fig. 1. Pink numbers 1 and 2 represent phase 1 and 2 of changes in membrane potentials, respectively. Time scale (orange bars) = 100 s. Teal line in (*B*) represents the K2P1 inward Na^+ current recorded in 0 mM $[K^+]_e$ in the same CHO cell. The '*a*', '*b*', and '*c*' in (*C*) and (*D*) represent three types of whole-cell ramp currents described in Fig. 1. The '*b*' and '*c*' currents have reversal potentials of -18.7 ± 2.1 mV ($n = 20$) and -106.8 ± 3.3 mV ($n = 6$), respectively. *E*, representative resting membrane potentials (left) of CHO cells that expressed both Kir2.1 and K2P1 channels and showed classical two levels of resting membrane potential when Na^+-based bath solutions were first changed from 5 to 1 mM K^+ and then reversibly shifted to $NMDG^+$-based bath solutions with 1 mM K^+ (purple bar) and finally returned to Na^+-based bath solutions with 5 mM K^+. Whole-cell ramp currents (right) were measured before (solid and dashed red lines) and after (purple line) external Na^+ was replaced by equimolar $NMDG^+$ in bath solutions with 1 mM K^+.

the CHO cells exhibited two types of behaviours with respect to resting membrane potentials and background currents, which we also observed in Kir2.1-expressing human iPSC-derived cardiomyocytes and mouse HL-1 cardiomyocytes with ectopic expression of K2P1 channels. One subgroup of the CHO cells recapitulated classical two stable levels of resting membrane potential. These cells spontaneously depolarized to -19.0 ± 1.2 mV ($n = 49$) and then remained at this depolarization (Fig. 5*C*, top). Such depolarization could be ignited either before or after maximal hyperpolarization was reached in phase 1. Another population of the CHO cells spontaneously became depolarized to -21.7 ± 3.1 mV ($n = 16$) and then fluctuated between the two levels with various patterns (Fig. 5*D*, top). The first subgroup of the CHO cells showed '*a*' and '*b*' types of whole-cell ramp current, whereas the second subgroup displayed '*a*', '*b*' and '*c*' three types of whole-cell ramp current (Fig. 5*C* and *D*, bottom). Both subgroups of the CHO cells recapitulated the N-shaped *I–V* relationships with three zero-current potentials. The first and third zero-current potentials (-103.1 ± 1.5 mV; -19.1 ± 1.6 mV, $n = 19$) determined the two levels of resting membrane potential. Interestingly, the third zero-current potentials are ∼30 mV more positive than reversal potentials of K2P1 leak cation channels in 1 mM $[K^+]_e$. A linear combination of Kir2.1 and K2P1 ramp currents generates the N-shaped *I–V* relationships, and the third zero-current potentials are never more positive than the K2P1 reversal potentials. Thus, Kir2.1 and K2P1 currents counterbalance in a non-linear manner. CHO cells that were engineered to express both Kir2.1 and the mutant K2P1•T118I channels simply hyperpolarized to -106.5 ± 1.4 mV ($n = 28$) in 1 mM $[K^+]_e$.

We confirmed the contribution of K2P1 inward leak Na^+ currents to two levels of resting membrane potential by analysis of CHO cells expressing both Kir2.1 and K2P1 channels in 1 mM $[K^+]_e$. When external Na^+ was replaced with equimolar K2P1-impermeable $NMDG^+$, resting membrane potentials reversibly shifted from a depolarization of -18.5 ± 2.6 mV ($n = 12$) to a hyperpolarization of -96.5 ± 1.7 mV (Fig. 5*E*, left). Only '*c*' type ramp currents with a reversal potential of -98.6 ± 2.0 mV ($n = 8$) were observed in $NMDG^+$-based bath solutions, whereas '*a*' and/or '*b*' types of currents were observed in Na^+-based bath solutions (Fig. 5*E*, right). Thus, removal of K2P1 inward leak Na^+ currents eliminated both the N-shaped *I–V* relationships and two levels of resting membrane potential of the CHO cells.

We also investigated whether Kir2.1 and K2P1 currents balance and set up two levels of resting membrane potential of the CHO cells in 2.7 mM $[K^+]_e$. Some cells permanently switched from -81.5 ± 2.1 mV to -22.1 ± 7.1 mV ($n = 8$), whereas another group showed spontaneous fluctuation of resting membrane potentials between -88.7 ± 0.8 mV and -21.6 ± 2.6 mV ($n = 12$). Both groups of cells also exhibited N-shaped whole-cell ramp currents with three zero-current potentials. The third zero-current potentials (-18.2 ± 3.3 mV, $n = 5$) were more positive than reversal potentials (-65.5 ± 0.9 mV, $n = 4$) of K2P1 leak cation channels in 2.7 mM $[K^+]_e$. These results indicate that Kir2.1 currents non-linearly counterbalance comparable low $[K^+]_e$-induced K2P1 leak cation currents, produce the N-shaped *I–V* relationships with three zero-current potentials and set up two levels of resting membrane potential at subphysiological $[K^+]_e$. These resting membrane potentials either spontaneously jump from hyperpolarization to depolarization in an all-or-none way or show spontaneous fluctuation between hyperpolarization and depolarization.

Discussion

Ionic mechanism of two levels of resting membrane potential in human cardiomyocytes

In the present study, we provide evidence supporting the hypothesis that Kir2 currents counterbalance non-linearly inward background cation currents, such as low $[K^+]_e$-induced K2P1 leak cation currents, accounting for two levels of resting membrane potential of human cardiomyocytes at subphysiological $[K^+]_e$. In our first set of experiments, we showed that human iPSC-derived cardiomyocytes function similarly to human adult cardiomyocytes deficient in Kir2, and human iPSC-derived cardiomyocytes engineered to express Kir2.1 not only recapitulated two stable levels of resting membrane potential at subphysiological $[K^+]_e$, as observed previously in human adult cardiomyocytes and cardiac Purkinje fibres (Gadsby & Cranefield, 1977; McCullough *et al.* 1990), but also displayed the N-shaped *I–V* relationships with three zero-current potentials, as reported previously in cardiac Purkinje fibres (Gadsby & Cranefield, 1977). This result implies that Kir2 currents are required for the phenomenon of two levels of resting membrane potential. In support of this hypothesis, human adult ventricular cardiomyocytes express higher levels of Kir2 currents than do human adult atrial cardiomyocytes (Hibino *et al.* 2010) and two stable levels of resting membrane potential are more often observed in human adult atrial cardiomyocytes than in human adult ventricular cardiomyocytes at subphysiological $[K^+]_e$ (Ten Eick & Singer, 1979; McCullough *et al.* 1987; McCullough *et al.* 1990). In addition, the multiple types of cells that show the phenomenon of the two levels of resting membrane potential conduct Kir2 currents (Weidmann, 1956; Ellis, 1977; Gadsby & Cranefield, 1977; Miura *et al.* 1977; Lee & Fozzard, 1979; Ten Eick & Singer, 1979; Sheu *et al.* 1980; Gallin, 1981; Gallin & Livengood, 1981; Christe, 1982; Shah *et al.* 1987; Ravesloot *et al.* 1989; Sims & Dixon, 1989; McCullough

et al. 1990; Geukes Foppen *et al.* 2002; Struyk & Cannon, 2008; Jurkat-Rott *et al.* 2009).

Second, we demonstrated that K2P1 channels also contribute to the two levels of resting membrane potential of Kir2.1-expressing human iPSC-derived cardiomyocytes at subphysiological $[K^+]_e$. We are unable to distinguish whether these human iPSC-derived cardiomyocytes are atrial-like or ventricular-like because they become electrically quiescent and do not show pacemaker activity with distinct diastolic depolarization. In ∼75% of the iPSC-derived cardiomyocytes displaying the two levels of resting membrane potential, K2P1 leak currents are responsible for major inward cation currents, whereas other unknown cation currents are responsible for inward cation currents in the remainder of the cardiomyocytes. Inhibition of K2P1 expression using shRNA or removal of inward K2P-like Na^+ currents by replacement of external Na^+ with $NMDG^+$ eliminated the phenomenon of the two levels of resting membrane potential.

Our previous study indicated that K2P1 channels contribute to depolarized resting membrane potentials of human primary spherical cardiac myocytes at subphysiological $[K^+]_e$ (Ma *et al.* 2011*b*). These results are consistent with other two previous observations. K2P1 is detected in human hearts, but not mouse and rat hearts (Lesage *et al.* 1996; Lesage *et al.* 1997; Liu & Saint, 2004; Gaborit *et al.* 2007), and human cardiomyocytes, but not rat cardiomyocytes, show two levels of resting membrane potential (Bouchard *et al.* 2004). In human hearts, K2P1 is the most abundant in the atrium and then in cardiac Purkinje fibres and is moderately abundant in the ventricle (Ordog *et al.* 2006; Gaborit *et al.* 2007), consistent with the frequent observation of two stable levels of resting membrane potential in human cardiac Purkinje fibres and human cardiomyocytes (Christe, 1982; McCullough *et al.* 1990). Moreover, ectopic expression of K2P1 in mouse HL-1 cardiomyocytes resulted in two levels of resting membrane potential at subphysiological $[K^+]_e$.

Finally, Kir2.1-expressing human iPSC-derived cardiomyocytes display the same behaviours with respect to resting membrane potentials as CHO cells expressing both Kir2.1 and K2P1 channels, implying that there may be a common mechanism settling two levels of resting membrane potential. We propose that Kir2 currents counterbalance comparable opposing background cation currents, accounting for two levels of resting membrane potential observed in the cells investigated in the present study and other types of cells as well (Miyazaki *et al.* 1975; Sims & Dixon, 1989; Voets *et al.* 1996; Geukes Foppen *et al.* 2002; Struyk & Cannon, 2008).

There are several limitations in the present study. First, previous reports indicate that human adult cardiomyocytes depolarize to approximately −35 mV in 0.5–2.7 mM $[K^+]_e$ (Ten Eick & Singer, 1979; Christe, 1982; McCullough *et al.* 1990), whereas we observed depolarization of approximately −20 mV in CHO cells and human iPSC-derived cardiomyocytes engineered to express Kir2.1. This difference may be a result of different experimental conditions. Another possibility is that voltage-gated K^+ channels in human adult cardiomyocytes are open at above −35 mV and are involved in settling the third zero-current potential of the N-shaped currents. Second, we studied Kir2.1-mediated currents, whereas cardiac Kir2 currents are mediated by heteromeric Kir2.1/Kir2.x channels (Lopatin & Nichols, 2001; Anumonwo & Lopatin, 2010). However, Kir2.1 and cardiac Kir2 conductance shares the same strongly inward rectifying *I–V* relationships, and so Kir2.1 should play the same role as heteromeric channels in settling two levels of resting membrane potential. Third, other inward cation currents (e.g. Ca^{2+} currents) may counterbalance Kir2 currents (Wiggins & Cranefield, 1976). A fraction of Kir2.1-expressing human iPSC-derived cardiomyocytes deficient in K2P1 might conduct such cation currents. Fourth, quantitative analysis of the relative levels of outward Kir2 K^+ currents and K2P1 inward cation currents in transduced CHO cells showing two levels of resting membrane potential is very challenging for several reasons. Because measured whole-cell currents such as the N-shaped ramp currents are different from the linear combination of Kir2.1 and K2P1 currents, isolation of individual Kir2.1 and K2P1 currents in the same cells requires the successive application of specific blockers for both channels. However, specific blockers for K2P1 channels are not available. In addition, both outward Kir2 K^+ currents and K2P1 inward cation currents could be very small because previous studies have shown that K2P1 channels give rise to tiny currents when expressed in CHO cells, and we had to measure K2P1 cation currents in 0 mM $[K^+]_e$. Moreover, measurement of relative Kir2.1 and K2P1 currents at a certain test voltage may provide very little information on how such a complicated, dynamic balance between Kir2.1 and K2P1 currents occurs. Finally, we actually measured membrane potentials or maximal diastolic potentials of CHO cells and/or human iPSC-derived cardiomyocytes that express Kir2.1, which were used to mimic resting membrane potentials. Despite these limitations, our analysis clearly demonstrates that Kir2.1 and K2P1 channels reconstitute the phenomenon of two levels of resting membrane potential observed in cardiomyocytes.

Kir2 currents non-linearly counterbalance background cation currents, settling two levels of resting membrane potential

When Kir2 outward K^+ currents dominate K2P1 or other inward background or leak cation currents, CHO cells expressing both Kir2.1 and K2P1 channels, Kir2.1-expressing human iPSC-derived cardiomyocytes

and K2P1-expressing mouse HL-1 cardiomyocytes have a hyperpolarized resting membrane potential. These results are consistent with the observation that a fraction of human adult cardiomyocytes do not show two stable levels of resting membrane potential at subphysiological $[K^+]_e$ (Christe, 1982; McCullough *et al.* 1990). When Kir2 outward K^+ currents are comparable with K2P1 inward leak cation currents in test voltages between their reversal potentials, Kir2 and K2P1 currents counterbalance in a non-linear manner, generating N-shaped *I–V* relationships with three zero-current potentials, the hallmark for two levels of resting membrane potential that have been observed in multiple types of cells (Gadsby & Cranefield, 1977; Gallin & Livengood, 1981; Sims & Dixon, 1989). Furthermore, the counterbalances of these opposing comparable currents result in resting membrane potentials that spontaneously shift from hyperpolarization at the first zero-current potentials to all-or-none depolarization at the third zero-current potentials. Such N-shaped *I–V* relationships are much different from the linear combination of Kir2.1 and K2P1 ramp currents because the third zero-current potentials are more positive than reversal potentials of K2P1 leak cation channels. Our data suggest that Kir2 currents non-linearly balance other opposing cation currents, produce the N-shaped *I–V* relationships and settle two levels of resting membrane potential of other types of cells at physiological or subphysiological $[K^+]_e$.

References

Anumonwo JM & Lopatin AN (2010). Cardiac strong inward rectifier potassium channels. *J Mol Cell Cardiol* **48**, 45–54.

Bett GC, Kaplan AD, Lis A, Cimato TR, Tzanakakis ES, Zhou Q, Morales MJ & Rasmusson RL (2013). Electronic "expression" of the inward rectifier in cardiocytes derived from human-induced pluripotent stem cells. *Heart Rhythm* **10**, 1903–1910.

Bouchard R, Clark RB, Juhasz AE & Giles WR (2004). Changes in extracellular K^+ concentration modulate contractility of rat and rabbit cardiac myocytes via the inward rectifier K^+ current IK1. *J Physiol* **556**, 773–790.

Carmeliet E, Biermans G, Callewaert G & Vereecke J (1987). Potassium currents in cardiac cells. *Experientia* **43**, 1175–1184.

Chatelain FC, Bichet D, Douguet D, Feliciangeli S, Bendahhou S, Reichold M, Warth R, Barhanin J & Lesage F (2012). TWIK1, a unique background channel with variable ion selectivity. *Proc Natl Acad Sci U S A* **109**, 5499–5504.

Christe G (1982). Effects of low $[K^+]_o$ on the electrical activity of human cardiac ventricular and Purkinje cells. *Cardiovasc Res* **17**, 243–250.

Claycomb WC, Lanson NA, Jr., Stallworth BS, Egeland DB, Delcarpio JB, Bahinski A & Izzo NJ, Jr (1998). HL-1 cells: a cardiac muscle cell line that contracts and retains phenotypic characteristics of the adult cardiomyocyte. *Proc Natl Acad Sci U S A* **95**, 2979–2984.

Doss MX, Di Diego JM, Goodrow RJ, Wu Y, Cordeiro JM, Nesterenko VV, Barajas-Martinez H, Hu D, Urrutia J, Desai M, Treat JA, Sachinidis A & Antzelevitch C (2012). Maximum diastolic potential of human induced pluripotent stem cell-derived cardiomyocytes depends critically on I(Kr). *PloS ONE* **7**, e40288.

Eisner DA & Lederer WJ. (1979*a*). Inotropic and arrhythmogenic effects of potassium-depleted solutions on mammalian cardiac muscle. *J Physiol* **294**, 255–277.

Eisner DA & Lederer WJ (1979*b*). The role of the sodium pump in the effects of potassium-depleted solutions on mammalian cardiac muscle. *J Physiol* **294**, 279–301.

Ellis D (1977). The effects of external cations and ouabain on the intracellular sodium activity of sheep heart Purkinje fibres. *J Physiol* **273**, 211–240.

Gaborit N, Le Bouter S, Szuts V, Varro A, Escande D, Nattel S & Demolombe S (2007). Regional and tissue specific transcript signatures of ion channel genes in the non-diseased human heart. *J Physiol* **582**, 675–693.

Gadsby DC & Cranefield PF (1977). Two levels of resting potential in cardiac Purkinje fibers. *J Gen Physiol* **70**, 725–746.

Gallin EK (1981). Voltage clamp studies in macrophages from mouse spleen cultures. *Science* **214**, 458–460.

Gallin EK & Livengood DR (1981). Inward rectification in mouse macrophages: evidence for a negative resistance region. *Am J Physiol Cell Physiol* **241**, C9–C17.

Geukes Foppen RJ, van Mil HG & van Heukelom JS (2002). Effects of chloride transport on bistable behaviour of the membrane potential in mouse skeletal muscle. *J Physiol* **542**, 181–191.

Goldstein SA (2011). K2P potassium channels, mysterious and paradoxically exciting. *Science Signaling* **4**, pe35.

Goldstein SA, Bayliss DA, Kim D, Lesage F, Plant LD & Rajan S (2005). International Union of Pharmacology. LV. Nomenclature and molecular relationships of two-P potassium channels. *Pharmacol Rev* **57**, 527–540.

Grundy D (2015). Principles and standards for reporting animal experiments in the journal of physiology and experimental physiology. *J Physiol* **593**, 2547–2549.

Hibino H, Inanobe A, Furutani K, Murakami S, Findlay I & Kurachi Y (2010). Inwardly rectifying potassium channels: their structure, function, and physiological roles. *Physiol Rev* **90**, 291–366.

Hoekstra M, Mummery CL, Wilde AA, Bezzina CR & Verkerk AO (2012). Induced pluripotent stem cell derived cardiomyocytes as models for cardiac arrhythmias. *Front Physiol* **3**, 346.

Jurkat-Rott K, Weber MA, Fauler M, Guo XH, Holzherr BD, Paczulla A, Nordsborg N, Joechle W & Lehmann-Horn F (2009). K^+-dependent paradoxical membrane depolarization and Na^+ overload, major and reversible contributors to weakness by ion channel leaks. *Proc Natl Acad Sci U S A* **106**, 4036–4041.

Karakikes I, Ameen M, Termglinchan V & Wu JC (2015). Human induced pluripotent stem cell-derived cardiomyocytes: insights into molecular, cellular, and functional phenotypes. *Circ Res* **117**, 80–88.

Lee CO & Fozzard HA (1979). Membrane permeability during low potassium depolarization in sheep cardiac Purkinje fibers. *Am J Physiol Cell Physiol* **237**, C156–C165.
Lesage F, Guillemare E, Fink M, Duprat F, Lazdunski M, Romey G & Barhanin J (1996). TWIK-1, a ubiquitous human weakly inward rectifying K^+ channel with a novel structure. *Embo J* **15**, 1004–1011.
Lesage F, Lauritzen I, Duprat F, Reyes R, Fink M, Heurteaux C & Lazdunski M (1997). The structure, function and distribution of the mouse TWIK-1 K^+ channel. *FEBS Lett* **402**, 28–32.
Lieu DK, Fu JD, Chiamvimonvat N, Tung KC, McNerney GP, Huser T, Keller G, Kong CW & Li RA (2013). Mechanism-based facilitated maturation of human pluripotent stem cell-derived cardiomyocytes. *Circ Arrhythm Electrophysiol* **6**, 191–201.
Liu W & Saint DA (2004). Heterogeneous expression of tandem-pore K^+ channel genes in adult and embryonic rat heart quantified by real-time polymerase chain reaction. *Clin Exp Pharmacol Physiol* **31**, 174–178.
Lopatin AN & Nichols CG (2001). Inward rectifiers in the heart: an update on I(K1). *J Mol Cell Cardiol* **33**, 625–638.
Ma J, Guo L, Fiene SJ, Anson BD, Thomson JA, Kamp TJ, Kolaja KL, Swanson BJ & January CT (2011*a*). High purity human-induced pluripotent stem cell-derived cardiomyocytes: electrophysiological properties of action potentials and ionic currents. *Am J Physiol Heart Circ Physiol* **301**, H2006–H2017.
Ma L, Zhang X & Chen H (2011*b*). TWIK-1 two-pore domain potassium channels change ion selectivity and conduct inward leak sodium currents in hypokalemia. *Sci Signal* **4**, ra37.
McCullough JR, Baumgarten CM & Singer DH (1987). Intra- and extracellular potassium activities and the potassium equilibrium potential in partially depolarized human atrial cells. *J Mol Cell Cardiol* **19**, 477–486.
McCullough JR, Chua WT, Rasmussen HH, Ten Eick RE & Singer DH ((1990). Two stable levels of diastolic potential at physiological K^+ concentrations in human ventricular myocardial cells. *Circ Res* **66**, 191–201.
Miura DS, Hoffman BF & Rosen MR (1977). The effect of extracellular potassium on the intracellular potassium ion activity and transmembrane potentials of beating canine cardiac Purkinje fibers. *J Gen Physiol* **69**, 463–474.
Miyazaki SI, Ohmori H & Sasaki S (1975). Action potential and non-linear current–voltage relation in starfish oocytes. *J Physiol* **246**, 37–54.
Ordog B, Brutyo E, Puskas LG, Papp JG, Varro A, Szabad J & Boldogkoi Z (2006). Gene expression profiling of human cardiac potassium and sodium channels. *Int J Cardiol* **111**, 386–393.
Rajan S, Plant LD, Rabin ML, Butler MH & Goldstein SA (2005). Sumoylation silences the plasma membrane leak K^+ channel K2P1. *Cell* **121**, 37–47.
Rastegar A & Soleimani M (2001). Hypokalaemia and hyperkalaemia. *Postgrad Med J* **77**, 759–764.
Ravesloot JH, Ypey DL, Vrijheid-Lammers T & Nijweide PJ (1989). Voltage-activated K^+ conductances in freshly isolated embryonic chicken osteoclasts. *Proc Natl Acad Sci U S A* **86**, 6821–6825.
Shah AK, Cohen IS & Datyner NB (1987). Background K^+ current in isolated canine cardiac Purkinje myocytes. *Biophys J* **52**, 519–525.
Sheu SS, Korth M, Lathrop DA & Fozzard HA (1980). Intra- and extracellular K^+ and Na^+ activities and resting membrane potential in sheep cardiac purkinje strands. *Circ Res* **47**, 692–700.
Sims SM & Dixon SJ (1989). Inwardly rectifying K^+ current in osteoclasts. *Am J Physiol Cell Physiol* **256**, C1277–C1282.
Struyk AF & Cannon SC (2008). Paradoxical depolarization of BA^{2+}- treated muscle exposed to low extracellular K^+: insights into resting potential abnormalities in hypokalemic paralysis. *Muscle Nerve* **37**, 326–337.
Ten Eick RE & Singer DH (1979). Electrophysiological properties of diseased human atrium. I. Low diastolic potential and altered cellular response to potassium. *Circ Res* **44**, 545–557.
Voets T, Droogmans G & Nilius B (1996). Membrane currents and the resting membrane potential in cultured bovine pulmonary artery endothelial cells. *J Physiol* **497**, 95–107.
Weidmann S (1956). *Elektrophysiologie der Herzmuskelfaser*, Huber, Bern.
Wiggins JR & Cranefield PF (1976). Two levels of resting potential in canine cardiac Purkinje fibers exposed to sodium-free solutions. *Circ Res* **39**, 466–474.
Zaza A (2009). Serum potassium and arrhythmias. *Europace* **11**, 421–422.

Additional information

Competing interests

The authors declare that they have no competing interests.

Author contributions

DZ and KC performed the experiments and participated in the analysis of data, design of figures and the writing of the paper. DZ, KC, MZ and ZL participated in design of the experiments. HC participated in design of the experiments and analysis of data, wrote the paper and supervised the project.

Funding

This work was supported by the National Institute of General Medical Sciences (R01GM102943), the American Heart Association (11GRNT7270014), and the National Natural Science Foundation of China (81370296 and 81370297) and Shanghai Pujiang Program (15PJ1406900).

Acknowledgements

We thank William C. Claycomb for providing cultured HL-1 cardiomyocytes.